

Proactive-cooperative Navigation in Human-like Environment for Autonomous Robots

Wanting Jin^a, Paolo Salaris^b and Philippe Martinet^c

Chorale Team, INRIA Sophia Antipolis, Valbonne, France

Keywords: Human-robot Interaction, Proactive Planning, Cooperative Behavior, Social Force Model.

Abstract: This work¹ deals with the problem of navigating a robot in a constrained human-like environment. We provide a method to generate a control strategy that enables the robot to proactively move in order to induce desired and socially acceptable cooperative behaviors in neighboring pedestrians. Contrary to other control strategies that simply aim to passively avoid neighboring pedestrians, this approach aims to simplify the navigation task of a robot by looking for cooperation with humans, especially in crowded and constrained environments. The co-navigation process between humans and a robot is formalized as a multi-objective optimization problem and a control strategy is obtained through the Model Predictive Control (MPC) approach. The Extended Headed Social Force Model with Collision Prediction (EHSFM with CP) is used to predict the human motion. Different social behaviors of humans when moving in a group are also taken into account. A switching strategy between purely reactive and proactive-cooperative planning depending on the evaluation of human intentions is also furnished. Validation of the proactive-cooperative planner enables the robot to generate more socially and understandable behaviors is done with different navigation scenarios.

1 INTRODUCTION

In order to enable the robot to establish a cooperative behavior with humans in a constrained environment, the robot not only should be able to plan its motion in the presence of humans but also to predict human actions. The problem has two main parts: *Human Aware Navigation* and *Human Motion Prediction*.

Human Aware Navigation. Reactive planning treats pedestrians as static or moving obstacles in the environment (Bevilacqua et al., 2018). However, proactive planning extends reactive planning by taking into account that humans can see the robot and react accordingly. In (Ferrer and Sanfeliu, 2019) authors propose an Anticipative Kino-dynamic Planner, where the reaction of the human towards robot motion has been taken into account. In (Truong and Ngo, 2017), the robot motion is planned by using the Hybrid Reciprocal Velocity Obstacle (Snape et al., 2011), which is known as a proactive velocity-based approach.

However, in previous works, human motion is only a passive reaction to the robot one. It is worth noting that besides passively move to avoid the collision, humans are also able to understand others' navigation intentions and actively move to give convenience to others. In (Che et al., 2020), the robot expresses its navigation desire through explicit and implicit communication. In (Khambhaita and Alami, 2020), both human and robot trajectories are optimized during the cooperation process.

Human Motion Prediction. The microscopic human motion model can be roughly classified as physics-based, planning-based and learning-based. For the planning-based methods, humans behave like planners by finding an optimal path during navigation (Mombaur et al., 2010). In (Trautman et al., 2013), human motion is modeled as an Interacting Gaussian Process. However, such methods require a lot of data for training and do not generalize to different environments. Among the physics-based models, the Social Force Model (SFM) is the most used one (Helbing and Molnár, 1995) which is a simple and universal method that could provide valid motion predictions by taking into account the interactions with the environment. In the case of cooperation, human behaviors are not only based on the information per-

^a <https://orcid.org/0000-0002-3399-0499>

^b <https://orcid.org/0000-0003-1313-5898>

^c <https://orcid.org/0000-0001-5827-0431>

¹This work is funded by MOBI-DEEP project (ANR-17-CE33-0011) and CROWDBOT project (H2020 n.779942).

ceived from surrounding but also depend on their intentions. In (Tamura et al., 2012), the sub-goals are set based on human intentions. In (Zanlungo et al., 2011), the authors improve the initial SFM by adding the explicit collision prediction (CP). In this paper, we choose a suitable cost function and define a constrained optimization framework to generate both reactive and proactive-cooperative motions for a mobile robot in human-like environments. We extend the SFM framework and show by simulations that it is able to give reasonable and useful predictions of human motions, even during the cooperative phase. We also provide a switching strategy between reactive and proactive-cooperative planning depending on the human availability to collaborate. Finally, we test the performances of the proposed machinery under different and significant human-robot interaction scenarios, especially where the cooperation and the communication of intentions are important (Khambhaita and Alami, 2017).

2 NAVIGATION STRATEGY

In this section, our proactive-cooperative planning is described and the switching strategy for passing from purely reactive strategy to a proactive one is provided.

2.1 Multi-objective Optimization

For simplicity reasons, both humans and robots are modeled as cylinders with radius r_r and r_i , respectively. The configuration of the vehicle is described by $\mathbf{q}_r(t) = (\mathbf{p}_r(t), \theta_r(t))$, where $\mathbf{p}_r(t) = (x_r(t), y_r(t))^T$ is the position of the vehicle, and $\theta_r(t)$ is the vehicle heading angle. The input of the vehicle is denoted by $\mathbf{u}_r = [v_r(t), \omega_r(t)]^T$ with $v_r(t)$ and $\omega_r(t)$ the forward and angular velocity respectively. We also define $\mathbf{v}_r = \dot{\mathbf{p}}_r$ as the robot linear velocity. In this paper, we use a kinematic and nonholonomic model for our robot but any other model can be used. Let us also consider humans moving on the same plane around the robot and represent the state of the i -th person as $\mathbf{q}_i(t) = (\mathbf{p}_i(t), \theta_i(t), v_i^f(t), v_i^o(t), \omega_i(t))$, where $\mathbf{p}_i(t) = (x_i(t), y_i(t))^T$ and $\theta_i(t)$ are defined similar as the configuration of robot. And ω_i is the angular velocity. We will assume the following dynamic model for each person in the environment:

$$\begin{aligned} \dot{x}_i &= v_i^f \cos \theta_i - v_i^o \sin \theta_i; \dot{y}_i = v_i^f \sin \theta_i + v_i^o \cos \theta_i \\ \dot{\theta}_i(t) &= \omega_i; \dot{v}_i^f(t) = \frac{1}{m_i} u_i^f; \dot{v}_i^o(t) = \frac{1}{m_i} u_i^o; \dot{\omega}_i(t) = \frac{1}{I_i} u_i^\theta \end{aligned} \quad (1)$$

where $\mathbf{u}_i = [u_i^f, u_i^o, u_i^\theta]^T$ are the inputs used to generate the predicted trajectory. The mass and the inertia of the i -th person are defined as m_i and I_i . We define $\mathbf{v}_i = \dot{\mathbf{p}}_i$ as the human linear velocity expressed on the plan of motion.

The motion planning problem can be hence formalized as a constrained multi-objective optimization problem (see Sec. 4) that smoothly adapts to different social scenarios by changing the weights of the linear scalarization applied to the cost function. As a consequence, in a generic form, the constrained multi-objective optimization problem can be formalized as

$$\begin{aligned} \mathbf{u}_r^* &= \arg \min_{\mathbf{u}_r} \int_{\bar{t}}^{\bar{t}+T} \sum_{\mu} \gamma_{\mu} F_{\mu}(\mathbf{u}_r(\tau), \mathbf{q}_r(\tau), \mathbf{q}_1(\tau), \dots, \mathbf{q}_N(\tau)) d\tau \\ \text{s.t. } & \mathbf{g}(\mathbf{u}_r(t), \mathbf{q}_r(t), \dots, \mathbf{q}_N(t)) \leq 0 \end{aligned} \quad (2)$$

where \bar{t} is the current time, T is the whole horizon time, N is the total number of pedestrians in the neighborhood, γ_{μ} are the weights to be adapted depending on the current scenario, $F_{\mu}(\cdot)$ are the cost functions (see Sec. 4.1), $\mathbf{g}(\cdot)$ are the several constraints (see Sec. 4.2). As it will be clear in Sec. 4, the optimization problem (2) will be solved by adopting the Model Predictive Control (MPC).

2.2 Proactive-cooperative Planning

A reactive action consists in a local path corresponding to an instantaneous reaction to sensory feedback. An action can be defined instead as proactive if it has the ability of **creating** or **controlling** a situation rather than just responding to it after it happened. To be proactive a robot has to act with the aim of creating or controlling a situation that, e.g., may facilitate a subsequent phase of cooperation and/or the robot (human) objective. Differently from reactive planning, proactive one must take into account if the human is willing to cooperate or not by observing how he/she reacts. In the starting stage of the proactive-cooperative planning, the robot should proactively generate actions to express its willingness to cooperate and intentions clearly. Once the human understands the robot's objective and is willing to cooperate, the cooperation phase starts (see Figure 1). The main difference between reactive and proactive-cooperative planning is that, the latter updates the predicted human trajectory simultaneously with the planned robot trajectory. Hence, both human and robot future trajectories are taken into account for the optimization process (see the two-way arrows between the "Human State Prediction" and "Proactive-Cooperative Planning" blocks in Figure 1).

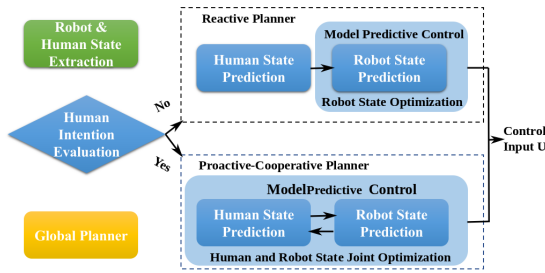


Figure 1: Local planning framework.

2.3 Switching Strategy

Based on previous analysis, it is clear that the robot must be able to switch between reactive and cooperative-proactive strategies depending on the result of the evaluation of human intentions. For simplicity reasons, we consider only two possible human intentions (denoted by int):

- iff $int = 0$: human does not see the robot or is not willing to cooperate;
- iff $int = 1$: human sees the robot and is willing to cooperate;

Let us introduce now the confidence of human intentions $Con_{int} = g(ms)$, as a function of ms which can be considered as the "measurement" of human reaction to robot movements. ms is defined as a binary function which depends on the difference between the observation of the real human trajectories \hat{q}_i^{real} and the predicted one during cooperation q_i^{coop} as:

- $ms = 0$: when $\|\hat{q}_i^{real} - q_i^{coop}\| > e_{thres}$
- $ms = 1$: when $\|\hat{q}_i^{real} - q_i^{coop}\| < e_{thres}$

where, e_{thres} is a threshold parameter.

$Odd(int) = \frac{p(int=1)}{p(int=0)}$ and $Odd(int|ms) = \frac{p(int=1|ms)}{p(int=0|ms)}$ are defined as the ratio between the possibility of having $int = 1$ and $int = 0$ before and after ms is updated. Its form can be simplified through Bayes rule and apply \log operator to both sides as

$$\log Odd(int|ms) = \log \frac{p(ms|int=1)}{p(ms|int=0)} + \log Odd(int) \quad (3)$$

We use the value of $\log Odd(int)$ to represents the confidence of human intentions Con_{int}^- before updating ms , and $\log Odd(int|ms)$ to represent the updated confidence Con_{int}^+ after updating ms . Previous equation (3) becomes $Con_{int}^+ = Con_{int}^- + lomeas$, with:

$$lomeas = \begin{cases} lonot = \log \frac{p(ms=0|int=1)}{p(ms=0|int=0)} \in (-1, 0) \\ loseee = \log \frac{p(ms=1|int=1)}{p(ms=1|int=0)} \in (0, 1) \end{cases} \quad (4)$$

where $lomeas$ is a predefined value indicating how the Con_{int} should be updated depending on the "measurement" ms . During the interaction process between the human and the robot, the robot will have a new ms at each time step, and Con_{int} will be updated continuously through the whole interaction process. To avoid jerky motion during switching, hysteresis is introduced. When the robot and a person meet, the robot is not sure about human intentions. The robot needs to clearly show its cooperative willingness and checks the human ones for cooperation. The confidence Con_{int} is initially set higher than a given confidence threshold Con_{thres-} , to enable the proactive-cooperative behavior. If the human responds to the robot motion accordingly then ms is set to 1 and the confidence Con_{int} keeps to increase and rests bigger Con_{thres+} : the cooperative process finally starts. If the human does not respond to robot suggestions or he/she decides to stop the cooperation then $ms = 0$, the confidence Con_{int} decreases and falls down Con_{thres-} . The robot switches to reactive planning to guarantee safety. During the reactive planning, if the confidence Con_{int} increases beyond Con_{thres+} , the robot switches again to the proactive-cooperative planning (Figure 2).

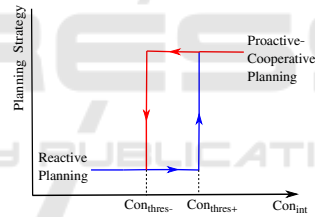


Figure 2: Switching strategy.

3 HUMAN MOTION

The robot needs to predict the human motion under different navigation scenarios. The Extended Headed Social Force Model (EHSFM) with Collision Prediction (CP) is proposed as a combination of three state of the art works built upon the SFM framework: The Headed Social Force Model (HSFM) (Farina et al., 2017), the Extended Social Force Model (ESFM) (Ferrer and Sanfeliu, 2019) and the collision prediction (CP) (Zanlungo et al., 2011).

3.1 Headed Social Force Model

The HSFM expands the SFM by taking into account that pedestrians usually move along its heading direc-

tion. The control input \mathbf{u}_i is hence computed as

$$\begin{aligned} \mathbf{u}_i^f &= \mathbf{f}_i^T \mathbf{e}_i^f \\ \mathbf{u}_i^o &= \beta^o (\mathbf{f}_i^e)^T \mathbf{e}_i^o - \beta^d v_i^o \\ \mathbf{u}_i^\theta &= -\beta^\theta (\theta_i - \theta_i^0) - \beta^\omega \omega_i \end{aligned} \quad (5)$$

Definitions of the parameters are the same as in (Farina et al., 2017). The interaction force between pedestrian i and agent z (z can be an obstacle o , a wall w and other pedestrians j) is

$$\mathbf{f}_{iz} = A_z e^{(r_{iz} - d_{iz})/B_z} \mathbf{n}_{iz} \quad (6)$$

where A_z reflects the strength of interaction, B_z corresponds to the interaction range. $r_{iz} = r_i + r_z$ is the sum of their radius. $d_{iz} = \|\mathbf{p}_i - \mathbf{p}_z\|$ denotes the distance between their centers. \mathbf{n}_{iz} denotes the normalized coordinates pointing from agent z to pedestrian i .

3.2 EHSFM with Collision Prediction

The EHSFM with CP extends the HSFM by including the ESFM to take into account the influence of robot motion on human one. The human ability of collision prediction is also added. The behaviors of humans when walking in a group are also introduced. Let \mathbf{u}_i the input as defined in 5. The definition of the social force is extended by introducing the effect of human-robot interactions, the range of view and the effects of people walking as a group. The total social force \mathbf{f}_i is

$$\mathbf{f}_i = \mathbf{f}_i^0 + \mathbf{f}_i^e + \mathbf{f}_i^{grp}. \quad (7)$$

In real cases, a group of people can separate for a while in order to avoid collision and then again come back in formation depending on the relationship between the members of the group (Bruneau et al., 2015). In our work, group behavior is modeled by considering a spring between a couple of people. When the members get closer or separate because of external force generated by the environment, the spring will push or bring them back to a comfortable distance. The group force and the stiffness of the spring s_g are defined as follows:

$$\begin{aligned} \mathbf{f}_i^{grp} &= s_g (d_{grp} - l_{grp}) \mathbf{n}_{ji} \\ \text{with } s_g &= \begin{cases} \kappa \frac{1 + \cos(\angle \mathbf{v}_i, \mathbf{v}_j)}{2l_{grp} e^{\|\mathbf{v}_i - \mathbf{v}_j\|}} & \text{if } d_{grp} < 2l_{grp} \\ 0 & \text{otherwise} \end{cases} \end{aligned} \quad (8)$$

where d_{grp} is the current distance between a couple of members and l_{grp} is the initial distance before the interaction with the robot. Parameter κ represents the relationship between two persons. Its value for a group of mother and son should be higher than for a group of friends. The stiffness of the spring should

reduce to model the intention of the member of separating each other, thus it is also a function of the difference between two members' heading direction and the magnitude of the velocity. When $d_{grp} > 2l_{grp}$ a couple of people are not treated as a group anymore.

The updated external force \mathbf{f}_i^e is defined as:

$$\begin{aligned} \mathbf{f}_i^e &= \sum_{j(\neq i) \in N} w_{\psi_{ij}} \mathbf{f}_{ij}^{CP} + \sum_{w \in W} w_{\psi_{iw}} \mathbf{f}_{iw}^{CP} \\ &+ \sum_{o \in O} w_{\psi_{io}} \mathbf{f}_{io}^{CP} + \sum_{r \in R} w_{\psi_{ir}} \mathbf{f}_{ir}^{CP} \end{aligned} \quad (9)$$

where N , O , R are the sets of pedestrians, obstacles and robots in the environment. $w_{\psi_{iz}}$ takes into account the anisotropy effect of the interaction force (Johansson et al., 2007) caused by the human's limit field of view and it is defined as:

$$w_{\psi_{iz}} = (\lambda + (1 - \lambda) \frac{1 + \cos(\psi_{iz})}{2}), \quad \cos(\psi_{iz}) = \mathbf{e}_i^f \cdot \mathbf{n}_{iz} \quad (10)$$

where ψ_{iz} is the angle between human forward direction \mathbf{e}_i^f and normalized distance vector \mathbf{n}_{iz} . $\lambda \in [0, 1]$ is a parameter which grows with the strength of interactions from behind.

The interaction force generated by the robot \mathbf{f}_{ir}^{CP} is added to model the effects of the robot motion on the human one. The interaction force \mathbf{f}_{iz} defined in (6) is not enough to model human intention during cooperation since it models human motion as a pure reaction to changes in the environment. In order to model the cooperative behavior between humans and the robot, the human's ability of Collision Prediction (CP) to solve potential collisions is taken into account. The interaction force with CP \mathbf{f}_{iz}^{CP} (z can be obstacles o , walls w , pedestrians j and robots r) is

$$\mathbf{f}_{iz}^{CP}(\{\mathbf{d}_{iz}\}, \{\mathbf{v}_{iz}\}, \mathbf{v}_i) = A_z' \frac{v_i}{t_i} e^{-d_{iz}/B_z'} \frac{\mathbf{d}'_{iz}(t_i)}{d'_{iz}(t_i)} \quad (11)$$

The parameters are defined similarly to (Zanlungo et al., 2011). The comparison between \mathbf{f}_{iz} and \mathbf{f}_{iz}^{CP} is showed in Figure 3. Under the scenario where agent i and j meet face to face in a corridor, \mathbf{f}_{ij} is along continuous lines which depend on the current relative positions. This leads both agents to decelerate but cannot generate significant lateral motion until they are very close. \mathbf{f}_{ij}^{CP} is instead along the dashed lines which depend on the future point of potential collision. This leads the two agents to move in the lateral direction and gives the way to the others.

4 PROBLEM DEFINITION

The optimization problem is now formalized by using the MPC which solves an optimal control problem for

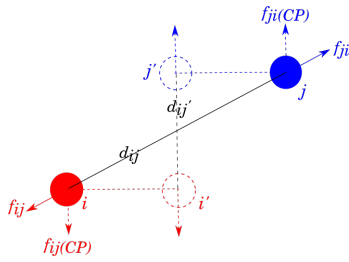


Figure 3: Comparison between f_{ij} and f_{ij}^{CP} when two agents i and j meet face to face in a corridor

a finite horizon time window T , using the state of the system of the current time \bar{t} as the initial state. The horizon time is hence divided into h steps of fixed length Δt , such that $h\Delta t = T$. k is then used to represent each time step with $k \in \{0, 1, \dots, h\}$.

Reactive Planning. For reactive planning, the robot motions do not influence the human ones. Thus, once the robot detects a person in the environment, it predicts the human future state by using HSFM and then modifies its own trajectory to avoid collisions. The optimization problem can be defined as:

$$\arg \min_{\{\mathbf{u}_r(0) \dots \mathbf{u}_r(h)\}} \sum_{k=0}^h \gamma_1 F_{goal}(k) + \gamma_2 F_{energy}(k) \quad (12)$$

s.t. Model: $\mathbf{q}_r(k+1) = \mathbf{q}_r(k) + \dot{\mathbf{q}}_r(\mathbf{u}_r(k))\Delta t$

Constraints: $g_1(k); g_2(k); g_4(k)$

$$\text{State feedback: } \begin{cases} \mathbf{q}_r(0) = \hat{\mathbf{q}}_r(\bar{t}) \\ \{\mathbf{q}_i(0) \dots \mathbf{q}_i(h)\} = \{\hat{\mathbf{q}}_i(\bar{t}) \dots \hat{\mathbf{q}}_i(\bar{t} + h)\} \end{cases}$$

Proactive-cooperative Planning. For proactive-cooperative planning, the robot not only needs to accomplish its navigation task as for the reactive planning but also to express its cooperation willingness clearly while, at the same time, maximizing the human comfort by respecting social rules. The predicted human trajectories and the robot ones are updated at the same time by using the EHSFM with CP. The optimization problem is defined as:

$$\arg \min_{\{\mathbf{u}_r(0) \dots \mathbf{u}_r(h)\}} \sum_{k=0}^h \gamma_1 F_{goal}(k) + \gamma_2 F_{energy}(k) + \gamma_3 F_{indiv}(k) + \gamma_4 F_{dir}(k) + \gamma_5 F_{ttc}(k) + \gamma_6 F_{group}(k) \quad (13)$$

s.t. Model: $\begin{cases} \mathbf{q}_r(k+1) = \mathbf{q}_r(k) + \dot{\mathbf{q}}_r(\mathbf{u}_r(k))\Delta t \\ \mathbf{q}_i(k+1) = \mathbf{q}_i(k) + \dot{\mathbf{q}}_i(\mathbf{q}_i(k), \mathbf{q}_r(k))\Delta t \end{cases}$

Constraints: $g_1(k); g_2(k); g_3(k); g_4(k); g_5(k)$

$$\text{State feedback: } \begin{cases} \mathbf{q}_r(0) = \hat{\mathbf{q}}_r(\bar{t}) \\ \mathbf{q}_i(0) = \hat{\mathbf{q}}_i(\bar{t}) \end{cases}$$

4.1 Cost Function

In (12) and (13), the cost function is composed of:

Reach the Goal. The robot has to reach a given goal or a close area around it.

$$F_{goal}(k) = \left\| \mathbf{p}_r(k) - \mathbf{p}_r^{goal}(\bar{t}) \right\|^2 \quad (14)$$

Energy Consuming. The energy at each time step k :

$$F_{energy}(k) = \|\mathbf{u}_r(k)\|^2 \quad (15)$$

Individual Comfort. The influence of the robot motion on each person is modeled by the interaction force. The cost function for individual comfort is:

$$F_{indiv}(k) = \left\| \mathbf{f}_{ir}^{CP}(k) \right\|^2 \quad (16)$$

Group Comfort. The cost to separate or compress the group because of robot motion can be formalized by the potential energy of the spring in the group:

$$F_{group}(k) = \frac{1}{2} s_g (d_{grp}(k) - l_{grp})^2 \quad (17)$$

Directionality. The directional cost function penalizes the face to face behavior between humans and the robot to increase the legibility of robot motion. The evaluation parameter of directional cost is (Khambhaita and Alami, 2020)

$$c_{dir}(k) = \frac{\mathbf{v}_r(k) \cdot \overrightarrow{\mathbf{p}_r \mathbf{p}_i}(k) + \mathbf{v}_i(k) \cdot \overrightarrow{\mathbf{p}_i \mathbf{p}_r}(k)}{C(k)^2} \quad (18)$$

where C is the distance between robot and human i . The penalty cost function for directionality is $F_{dir}(k)$

$$= \begin{cases} (\zeta_{dir} + \epsilon) - c_{dir}(k) & \text{if } c_{dir}(k) < (\zeta_{dir} + \epsilon) \\ 0 & \text{otherwise} \end{cases} \quad (19)$$

where ζ_{dir} is a threshold of activation, ϵ is a parameter that takes into account the accuracy of the directional estimation. Notice that, higher relative velocity and shorter distance means a higher penalty. The directional cost function sets up the trade-off between the effect of slowing down and changing the path.

Time to Collision. The robot is expected to look ahead and anticipate its actions clearly. The minimum distance between the robot and human i in a future time window η is

$$d_{ttc}(k) = \min_{t_m \in (0, \eta)} \left\| (\mathbf{p}_r + \mathbf{v}_r t_m) - (\mathbf{p}_i + \mathbf{v}_i t_m) \right\|^2 \quad (20)$$

while the cost function corresponding to the minimum human-robot distance within η is

$$F_{ttc}(k) = \begin{cases} \frac{(\rho_{ttc} + \epsilon) - d_{ttc}(k)}{C(k)^2} & \text{if } d_{ttc}(k) < (\rho_{ttc} + \epsilon) \\ 0 & \text{otherwise} \end{cases} \quad (21)$$

If d_{ttc} is smaller than a certain threshold ρ_{ttc} , then the cost function is activated and, if minimized, pushes the robot to move sideways in head of time η . Therefore, the robot clearly suggests a solution to the human on how reducing the risk of a potential collision.

4.2 Constraint

The constraints that guarantee safety and comfort are: **Proxemic constraint.** The proxemics theory introduced in (Twitchell Hall, 1966) defines areas around people with different distances of interaction w.r.t. the others, e.g. the intimate space is within $0.45m$ and the personal space is within $1.2m$. Since the scenario for our task is extremely constrained, the robot may go into the pedestrian's personal space but it should never violate the intimate space to guarantee comfort. Thus, the distance between pedestrian i (with $i \in N$) and the robot should be bigger than the intimate space radius ξ_{per} , i.e.

$$g_1(k) : r_r + r_i + \xi_{per} - \|\mathbf{p}_r(k) - \mathbf{p}_i(k)\| < 0 \quad (22)$$

Safety Distance Constraint to Walls. The robot should stay sufficiently far from walls. The walls are defined as line segments in 2D. The distance d_{rw_i} between each wall w (with $w \in W$) and the robot must be bigger than the safety distance ξ_{wall} . Moreover, the robot motion should not push the human i too close to the wall. Thus, these constraints are:

$$g_2(k) : r_r + \xi_{wall} - d_{rw}(k) < 0 \quad (23)$$

$$g_3(k) : r_i + \xi_{wall} - d_{iw}(k) < 0 \quad (24)$$

Safety Distance Constraint to Obstacles. Each obstacle is defined as a circumscribing disc-shaped object with center position \mathbf{p}_o and radius r_o . The definition of safety constraint to obstacles are similar to safety constraint to walls.

$$g_4(k) : r_r + \xi_{obs} - d_{ro}(k) < 0 \quad (25)$$

$$g_5(k) : r_i + \xi_{obs} - d_{io}(k) < 0 \quad (26)$$

5 RESULTS AND ANALYSIS

Simulations are done in Matlab[®]. The total simulation time is 10s. The size of the horizon time window is $T = 5s$. At each time step, the future control input consists of a sequence of 10 piece-wise constant values. As a consequence, $\Delta t = 0.1s$. Three scenarios of interactions between one single person and one single robot have been considered. *Scenario 1:* one single person and one robot meet face to face in a corridor; *Scenario 2:* one single person and one robot perform a 90° path-crossing; *Scenario 3:* as in scenario 1 with an obstacle partially blocking the way. For these scenarios, a comparison between reactive and proactive-cooperative planning has been done. Finally, in *Scenario 4* one robot meets a group of persons.

Model Parameter. As mentioned in (Khambhaita and Alami, 2017), the parameter re-tuning or learning under different scenarios is required for every state of the art human motion prediction method since humans behave differently in different situations. The parameters used in each scenario (see Table 1) are tuned manually. More reasonable values can be learned through data analysis of real experiments (Ferrer and Sanfeliu, 2019) in future works.

Table 1: Parameters of Human Motion Model.

Scenario N°	A'_r	B'_r	A'_o	B'_o	A'_w	B'_w	A'_w	B'_w
(1)	250	6	250	6	0	0	2000	0.08
(2)	250	15	250	15	0	0	2000	0.08
(3)	250	12	250	12	400	0.5	2000	0.08
(4)	250	6	250	6	0	0	2000	0.08
(5)	250	6	250	6	0	0	2000	0.08

Optimization Parameters. The weighting parameters and penalty thresholds for each cost function need to be re-tuned for each scenario in order to have proper behavior. The parameters used in this paper are in Table 2. The proxemics distance is set to $\xi_{per} = 0.45$ m. The safety distance between human (robot) and the wall and the obstacle are set to $\xi_{wall} = 0.2$ m, $\xi_{obs} = 0.1$ m. The collision time window is set to $\eta = 8$ s.

Table 2: Weighting Parameters and Penalty Thresholds.

Scenario N°	γ_1	γ_2	γ_3	γ_4	γ_5	γ_6	ζ_{dir}	ρ_{tc}
(1)	1	1	0.005	200	200	0	0.5	2
(2)	0.1	1	0.05	100	100	0	1	1
(3)	1	1	0.05	100	100	0	0.5	2
(4)	1	1	0.005	200	200	0	0.5	2
(5)	1	1	0	100	100	1	0.5	2

Human and Robot Characteristic. Human mass is 75 kg and inertia $I_i = 0.045$ kg m². Humans radius is $r_i = 0.3$ m. We assume that humans reach the desired velocity of 1.5 m/s in $\phi = 0.5$ s. Robot radius is 0.3 m. The linear velocity $v_r \in [0, 2]$ and angular velocity $w_r \in [-1, 1]$.

Environment Parameters. The origin of the world reference frame is fixed at the bottom left corner of the wall on the left, with x_w and y_w axis along with the horizontal and vertical directions, respectively. The length and width of the corridor are 15 m and 5 m, respectively. The 90° cross path takes place in a square of 15×15 m.

5.1 Simulation Results

The simulation results are reported in Figure 4. The red (denoted by G_r) and blue (denoted by G_{hAct}) squares mark the position of the robot and human actual goal, respectively. In order to introduce some noise in the human motion prediction, the predicted

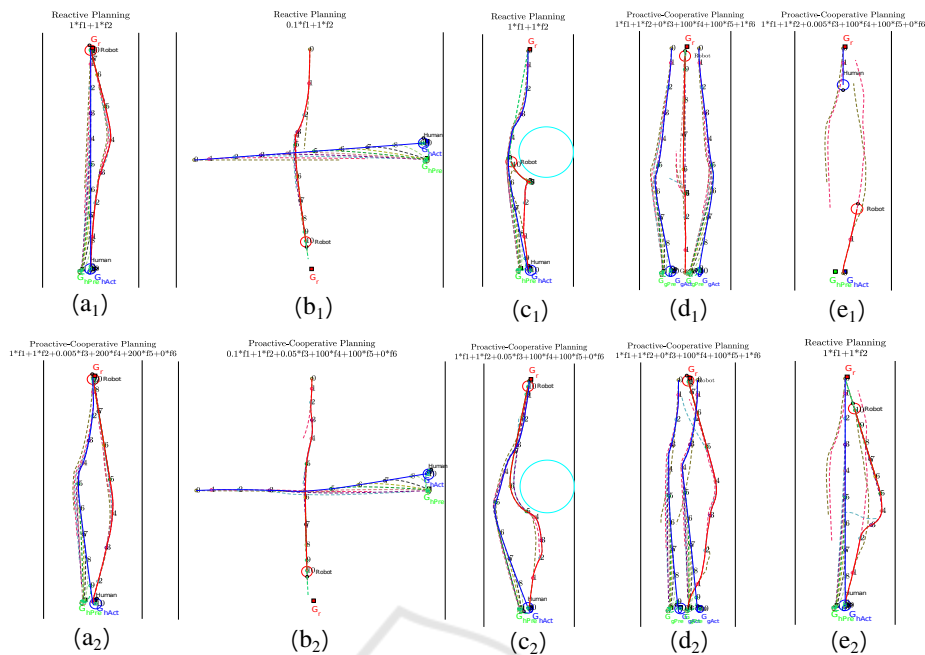


Figure 4: Simulation results for the four scenarios (a,b,c,d): Reactive (above) and proactive-cooperative (below); Switching strategy (e): 0-2s proactive-cooperative planning (above) and 3-10s reactive planning (below).

human navigation goal is set differently and marked with a green square (denoted by G_{hPre}). The red and the blue continuous curves (dashed curves) are then executed (planned) robot trajectory and the simulated (predicted) human trajectory, respectively. The colored circles on the red and blue continuous curves represent the robot and human positions at each second (with the number indicate the time).

Scenario 1. The human starts at the top middle of the corridor and plans to cross the corridor and reach his/her goal at the bottom middle (see Figure 4-(a)). The robot starts at the opposite position of the corridor and plans to reach the top middle of the corridor. The predicted human goal is $0.5m$ left of the actual goal. For the reactive planner, the robot detours to respect proxemics distance when it is close to the human. This may make human confused and threatened by the robot motion. By using proactive-cooperative planning (see Figure 4-(a), bottom), the robot decelerates while approaching the human and deviates to the lateral side to clearly show its cooperative intentions to the human. After the interaction, the robot accelerates again to reach its goal. Hence, the trajectory generated by our proactive-cooperative planning has higher legibility and is more socially acceptable.

Scenario 2. The human starts at the left middle of the square and plan to reach the right middle. The robot starts at the top middle of the square and plans to reach the bottom middle. The predicted human goal is $0.5m$ above the actual goal. By using reactive plan-

ning, the robot starts with high speed and then slows down and detours on the back of the human (almost at 4 s of the simulation). On the contrary, by using proactive-cooperative planning (see Figure 4-(b), bottom), the robot slows down initially as well as moving straight towards its navigation goal to show its intentions and let the human pass first. Once human passes the crossing point, the robot accelerates to reach his goal. During the interaction process, no confusion seems to be generated as the robot shows its navigation goal clearly and human accelerates to pass the crossing point and gives the way to the robot.

Scenario 3. The obstacle is a cylinder with center at $p_o = [3.5, 8]^T$ and radius $r_o = 1.5m$. Since the robot assumes the human will not give the way, during the time window 3s-8s the robot cannot find a feasible trajectory to reach the goal (see Figure 4-(c)). The robot has to turn around and move to the right side to respect the proxemic constraint during the time window 5s-6s. Indeed, the predicted human trajectories are different from real ones. By using our proactive-cooperative planning (see Figure 4-(c) bottom), the robot reaches the navigation goal much more efficiently. Moreover, it slows down and moves to the lateral side to clearly express its politeness. The human passes first the bottleneck created by the obstacle and gives enough space to the robot that clearly expressed to the human its navigation goal.

Scenario 4. The navigation scenario is as for Scenario 1. For the group of mother and son (see Fig-

ure 4-(d) bottom), $\kappa = 100$ and $l_{gr} = 1$ m. For the group of friends (see Figure 4-(d) top), $\kappa = 10$ and $l_{gr} = 2$ m. For the first case, when the robot meets a group of mother and son, since the spring stiffness is very high and may cost much energy to separate them, the robot detours from outside. However, in the second case, when the robot meets a group of friends, the robot passes through the group to save energy.

Switching strategy. The result for the corridor scenario is showed in Figure 4-(e). All the parameters for reactive and proactive-cooperative planner are fixed to correctly compare the performance of these two strategies. In real application, for reactive planning, the robot motion should be more conservative, with $v_r \in (0, 1]$ and the proxemic distance $\xi_{per} = 1.2$ m. For the switching parameters, the initial confidence $Con_{int} = 20$, $Con_{thres+} = 10$, $Con_{thres-} = 7$, $e_{thres} = 1$, $l_{not} = 2$ and $l_{see} = 1$. In Figure 4-(f) on the top, at the beginning the robot proactively communicates with the human its willingness. During this phase, the robot evaluates human intentions. Until 2s of simulation, the confidence Con_{int} is still beyond the threshold Con_{thres-} , thus the robot maintains a proactive and cooperative behavior. However, in the following (see Figure 4-(f) bottom), the real human trajectory differentiates from the predicted one, thus Con_{int} falls below the confidence threshold Con_{thres-} : the robot switches to reactive planning to guarantee safety.

6 CONCLUSIONS

A Proactive-cooperative planning for a mobile robot and a switching strategy to pass from a purely reactive to a proactive behavior depending on the confidence about human intentions is provided. Simulations show the effectiveness of our method. The many parameters introduced for modeling the human motion model in different situations are the main drawback of our method. Future works will be dedicated to include some learning strategies (e.g. (Ferrer and Sanfeliu, 2019) and (Che et al., 2020)) to determine these parameters and automatically adapt the method to any situation. Moreover, a simulator for taking into account more realistic human motions will be considered. Finally, real experiments are required to definitely validate the proposed machinery.

REFERENCES

Bevilacqua, P., Frego, M., et al. (2018). Reactive planning for assistive robots. *IEEE Robotics and Automation Letters*, 3(2):1276–1283.

- Bruneau, J., Olivier, A., and Pettré, J. (2015). Going through, going around: A study on individual avoidance of groups. *IEEE Trans. on Visualization and Computer Graphics*, 21(4):520–528.
- Che, Y., Okamura, A. M., and Sadigh, D. (2020). Efficient and trustworthy social navigation via explicit and implicit robot–human communication. *IEEE Transactions on Robotics*, pages 1–16.
- Farina, F., Fontanelli, D., et al. (2017). Walking ahead: The headed social force model. *PLOS ONE*, 12(1):1–23.
- Ferrer, G. and Sanfeliu, A. (2019). Anticipative kinodynamic planning: Multi-objective robot navigation in urban and dynamic environments. *Autonomous Robots*, 43(6):1473–1488.
- Helbing, D. and Molnár, P. (1995). Social force model for pedestrian dynamics. *Physical Review E*, 51:4282–4286.
- Johansson, A., Helbing, D., and Shukla, P. K. (2007). Specification of the social force pedestrian model by evolutionary adjustment to video tracking data. *Advances in Complex Systems*, 10:271–288.
- Khambhaita, H. and Alami, R. (2017). Assessing the social criteria for human-robot collaborative navigation: A comparison of human-aware navigation planners. In *Proc. IEEE ISRHIC*, pages 1140–1145.
- Khambhaita, H. and Alami, R. (2020). Viewing robot navigation in human environment as a cooperative activity. In *Robotics Research*, pages 285–300.
- Mombaur, K., Truong, A., and Laumond, J.-P. (2010). From human to humanoid locomotion—an inverse optimal control approach. *Autonomous Robots*, 28(3):369–383.
- Snape, J., van den Berg, J. P., et al. (2011). The hybrid reciprocal velocity obstacle. *IEEE Transactions on Robotics*, 27:696–706.
- Tamura, Y., Le, P. D., et al. (2012). Development of pedestrian behavior model taking account of intention. In *IEEE/RSJ IROS*, pages 382–387.
- Trautman, P., Ma, J., et al. (2013). Robot navigation in dense human crowds: the case for cooperation. In *Proc. IEEE ICRA*, pages 2153–2160.
- Truong, X. and Ngo, T. D. (2017). Toward socially aware robot navigation in dynamic and crowded environments: A proactive social motion model. *IEEE TASE*, 14(4):1743–1760.
- Twitchell Hall, E. (1966). *The hidden dimension*. Garden City, N.Y., Doubleday.
- Zanlungo, F., Ikeda, T., and Kanda, T. (2011). Social force model with explicit collision prediction. *EPL (Europhysics Letters)*, 93:68005.